AUTHOR QUERY FORM



Journal: J. Test. Eval.

Article Number: JTE20210205

Please provide your responses and any corrections by annotating this PDF and uploading it to ASTM's eProof website as detailed in the Welcome email.

Dear Author,

Below are the queries associated with your article; please answer all of these queries before sending the proof back to ASTM Production. Please contact ASTM at astmproduction@jjeditorial.com with any questions or concerns.

- 1. Please ensure accuracy of all affiliations, ORCID information, and spelling of all authors' names.
- 2. Please confirm corresponding author's email address and indicate if it has changed since submission. Note: only the corresponding author's email address will be included in the article.
- 3. Please review all tables and/or equations for accuracy.
- 4. Please thoroughly review all figures. If necessary, revised figures can be sent along with page proof corrections. Digital files can be attached to your annotated PDF.
- 5. Please provide email addresses for all authors. Complimentary PDFs of the final article will only be provided to authors with a valid email address. Please note that only the corresponding author's email address will be published.

Please respond to the following queries by clicking on the **AQ** link and inserting your comments or corrections as a PDF annotation. Additional comments can be left in the **Author Comments** column. We may require your response in order to proceed with production; unanswered queries may cause delays in publication.

Location in article	Query/Remark	Author Comments
AQ1	AQ: We note that while the author Cedric Sauzeat is intended to share the same affiliation as Herve di Benedetto, Sauzeat has departmental information (LTDS) provided at online submission that di Benedetto does not. If "LTDS" pertains to both authors, please add that information to the beginning of byline #4. If the "LTDS" information is unique to Sauzeat, please create a fifth affiliation for this author.	
AQ2	AQ: We note that the author "Cedric Sauzeat" is listed as "Cédric Sauzéat" at online submission. Please ensure that this author's name is correct in the manuscript file.	
AQ3	AQ: Please note that all author affiliations must include a complete street address per journal style. Please provide this information for affiliations #X and #	
AQ4	AQ: We note a discrepancy in the street address and the postal code in the manuscript file in affiliation #3 from the online submission system, where the address is listed as "W183 Kingsbury Hall" and the postal code is listed as "3824" Please review the affiliation in the manuscript file to ensure that all of its information is listed correctly.	
AQ5	AQ: We note that there are inconsistencies in the italicization of variables in your manuscript. Please carefully review all instances of variables in the text body and the equations and ensure all are correctly italicized. Please look particularly closely at "G" "E" and "δ" In the interim, all uses of these terms have been italicized. Please make edits as necessary based on ASTM's guidance, which states that all quantity symbols (variables) that can have a numerical or physical value should be italicized.	

AQ6	AQ: We note that the list of keywords in the manuscript file is considerably different from the list of	
	keywords submitted at the online submission system (asphalt materials, rheological measurements,	
	black space). Please review the keywords in the manuscript file to make sure the correct ones are used.	
AQ7	AQ: If "10C" is referring to a temperature, please edit to: "10°C"	
AQ8	AQ: "26.2 degrees" has been edited to "26.2°" If this is referring to temperature, please insert "C"	
	following the degree symbol if the temperature is Celsius. If referring to an angle, leave as is.	
AQ9	AQ: Please include the full definition of the abbreviation of PGLT upon first reference in the following	
	format: "[Full term] (PGLT)	
AQ10	AQ: Ref. 20 could not be verified. Please check and confirm the information given.	

Please confirm the following revisions by clicking on the C link and reviewing the revision. If you do not approve the change, please leave a comment or correction as a PDF annotation. Additional comments can be left in the **Author Comments** column. If you do not respond to the query, the change will be approved.

Location in article	Query/Remark	Author Comments
C1	C: We note that the author "Gordon D. Airey" is listed as "Gordon Airey" at online submission. Please ensure that this author's name is correct in the manuscript file.	
C2	C: We note that the author "Eshan V. Dave" is listed as "Eshan Dave" at online submission. Please check and confirm that this author is listed correctly in the manuscript file.	
C3	C: "Pavement Research Building" was added to the manuscript file for affiliation #1 based on information provided at online submission. Please check and confirm this change.	
C4	C: The ORCID for author Gordon D. Airey was added to the manuscript from the information pro- vided at submission. Please check and confirm this information.	
C5	C: The departmental information of "Department of Civil and Environmental Engineering" was added to affiliation #3 based on information provided at online submission. Please check and confirm this change.	
C6	C: The ORCIDs for authors Jo E. Sias and Eshan V. Dave were added to the manuscript from the information provided at submission. Please check and confirm this information.	
C7	C: We note that the institution in affiliation #4 is listed differently than it is in the online submission system, where it is listed as "Ecole Nationale des Travaux Publics de." Please review this affiliation and ensure it is correctly displayed in the manuscript file.	
C8	C: The street address provided in the online submission system (Rue Maurice Audin) has been added to the manuscript file for affiliation #4. Please check and confirm this change.	
С9	C: An abbreviated term must be used three times in order for the abbreviation to be retained in the main section of the manuscript. As such, the DMA abbreviation has been eliminated. Similar edits will be made as necessary.	
C10	C: The sentence beginning "This paper describes selected recent developments in the use of Black Space diagrams" has been reworded for clarity. Please review the sentence to ensure that its meaning was not changed.	
C11	C: The sentence beginning "Once the data are transformed" has been reworded for clarity. Please review the sentence to ensure that it's mean was not change.	
C12	C: The abbreviation "RAP has been defined as "reclaimed asphalt pavement" upon first reference. Please check and confirm this change.	

C13	C: Throughout the manuscript, dashes (-) have been swapped out for true negative signs (-) when it	
	appears a negative value is being expressed. Please check and confirm that this has been done properly	
	throughout the manuscript.	
C14	C: Because it only appeared once, the "MSCR" abbreviation has been expanded to "multiple stress	
	creep recovery test" Please check and confirm this change.	
C15	C: Because the abbreviation "PAV" was only used twice, it has been edited to "pressure aging vessel."	
	Please check and confirm this change.	
C16	C: The abbreviation "RTFOT" has been edited to" rolling thin-film oven test." Please check and con-	_
	firm this change.	
C17	C: The issue number was added to ref. 3. Please check and confirm this change.	
C18	C: Ref. 6 has been styled as a report. Additionally, only the first seven authors are now listed because of	
	ASTM rules that say "et al." should be used following the first seven authors when there are 11-plus	
	authors. Please check and confirm these changes.	
C19	C: The page range has been added to ref. 15. Please check and confirm this change.	
C20	C: The journal name has been edited and the page range added in ref. 16. Please check and confirm	
	this change.	
C21	C: ref. 17 has been styled as an unpublished conference proceeding. Please check and confirm this	
	change.	
C22	C: Ref. 21 has been styled as a presentation at a meeting. Please check and confirm this change.	
C23	C: The page range was added to ref. 25. Please check and confirm this change.	
C24	C: In ref. 27, the article ID number was added, and the journal article title was updated. Please check	
	and confirm these changes.	
C25	C: The sponsoring organization for the report in ref. 30 has been updated. Please check and confirm	
	this change.	
C26	C: The issue number was added to ref. 34. Please check and confirm this change.	
C27	C: The volume number in ref. 35 was edited. Please check and confirm this change.	



Complete this quote request and return by:

Email service@astm.org Fax +1.610.832.9555 Mail

ASTM International Attention: Inside Sales and Service 100 Barr Harbor Drive, PO Box C700 West Conshohocken, PA 19428-2959

Reprints Order Form

For reprints of articles and/or papers from ASTM Journals, Selected Technical Papers (STPs), book chapters, and *Standardization News*

Authors receive a 25% discount

C	hi	in	+-	
J	ш	ı	···	

Name	
Organization	
Address	
City	State Zip
Country	
Bill to:	
Name	
Organization	
Address	
City	State Zip
Country	
Reprint requesting:	
Paper Title	
Publication (title, month, and volume, STP, or stock number)	
Page length of article	Number of copies (25 minimum)
Cover (check one) Reprinted article, no cover Reprinted article	e and cover with typeset title of article and author's name
Date Tel	Email Fax



Reprints Price Scale

(Prices subject to change without notice)

Color Reprints

Pages/Copies	100	200	500	1,000	2,000
2	\$1,102	\$1,323	\$1,543	\$1,764	\$1,984
3-4	\$2,116	\$2,221	\$2,326	\$2,425	\$2,824
5-8	\$2,168	\$2,278	\$2,394	\$2,499	\$3,024
9-12	\$3,307	\$3,470	\$3,638	\$3,801	\$4,126

Black & White Reprints

Pages/Copies	25	50	100	200	300	500	1,000	2,000
1-4	\$136	\$152	\$168	\$184	\$199	\$226	\$310	\$472
5-8	\$195	\$226	\$257	\$278	\$299	\$352	\$499	\$709
9-12	\$225	\$257	\$289	\$336	\$357	\$425	\$577	\$787
13-16	\$263	\$294	\$325	\$394	\$430	\$520	\$751	\$1,118
17-20	\$278	\$336	\$394	\$472	\$514	\$635	\$887	\$1,307
21-24	\$301	\$373	\$446	\$535	\$583	\$724	\$1,003	\$1,475
25-28	\$331	\$404	\$478	\$583	\$646	\$808	\$1,165	\$1,795
29-32	\$383	\$441	\$299	\$651	\$724	\$913	\$1,323	\$2,058
Cover (optional)	\$100	\$115	\$136	\$157	\$178	\$220	\$373	\$598

ASTM International Inside Sales and Support department will contact you with a final price quote, including freight charges,



Journal of Testing and Evaluation

Gordon D. Airey,¹ Geoffrey M. Rowe,² Jo E. Sias,³ Herve Di Benedetto,⁴ Cedric Sauzeat,⁴ and Eshan V. Dave³

DOI: 10.1520/JTE20210205

Black Space Rheological Assessment of Asphalt Material Behavior



3

5

6 7

8

13

15

16

17

18

19

20

2.1

22

23

24

25

26

27

28

29

30

doi:10.1520/JTE20210205

available online at www.astm.org

Cedric Sauzeat, ⁴ and Eshan V. Dave ³
Black Space Rheological Assessment
of Asphalt Material Behavior

Gordon D. Airey, Geoffrey M. Rowe, Jo E. Sias, Herve Di Benedetto, 4

Reference

G. D. Airey, G. M. Rowe, J. E. Sias, H. Di Benedetto, C. Sauzeat, and E. V. Dave, "Black Space Rheological Assessment of Asphalt Material Behavior," Journal of Testing and Evaluation https://doi.org/10.1520/JTE20210205

Manuscript received March 26, 2021; accepted for publication September 22, 2021; published online xxxx xx, xxxx.

- ¹ NTEC, University of Nottingham, Pavement Research Building, Nottingham NG7 2RD, UK (Corresponding author), e-mail: gordon.airey@nottingham.ac.uk, https://orcid.org/0000-0002-2891-2517
- ² Abatech, PO Box 356, Blooming Glen. PA 18911. USA
- ³ Department of Civil and Environmental Engineering, University of New Hampshire, 33 Academic Way, Durham, NH 03824, USA, https://orcid. org/0000-0001-5284-0392 (J.E.S.), https://orcid.org/ 0000-0001-9788-2246 (E.V.D.)
- ⁴ University of Lyon/ENTPE, Rue Maurice Audin, Vaulx-en-Velin 69518, France

ABSTRACT

Black Space diagrams representing rheological data of asphalt materials in the form of complex modulus ($|G^*|$ or $|E^*|$) versus phase angle (δ) have been successfully used for interpretation of material behavior and performance. Previous studies have used Black Space for identification of testing geometry compliance errors when testing over multiple temperatures and loading times (frequencies), screening of the "thermo-rheological simplicity" of various binders and mixtures, and detailed evaluation of the performance balance in term of "stiffness" versus "relaxation" needs. This paper provides an overview of how Black Space can be further used to provide a greater understanding of the concepts of damage and healing and cracking susceptibility and fracture, and to also quantify the complex rheological response of alternative binders. In terms of the damage assessment, cyclic loading tests were analyzed using Black Space to identify additional physical phenomena such as nonlinearity, self-heating, and thixotropy. The cracking analysis has included thermal, fatigue, and durability cracking as well as the use of Black Space to access the performance of asphalt mixtures subjected to aging as well as rejuvenation and materials with recycled asphalt. Concepts such as the Glover-Rowe parameter that are based around Black Space and linked to other forms of rheological indices such as the low-temperature stiffness and relaxation rate parameters are introduced. The results in the paper show that Black Space provides a critical means of rheological characterization to investigate and evaluate the properties and performance of both binders and mixtures. This is particularly relevant at a time when there is a concerted move within the asphalt paving industry toward more sustainable solutions and increased demand for reuse and recycling of materials in asphalt mixtures.

Keywords

black space, rheology, cracking, damage, aging, rejuvenation, alternative binders

31 32

39

40

41

42

43

47

48

50

52

53

55

56

57

58

59

62

65

66

67

69

70

71

75

77

78

79

Introduction 33

The linear viscoelastic (LVE) characterization of asphalt materials has been extensively used in material selection, AQ6 mixture design, pavement design, and performance prediction. As a viscoelastic material, asphalt binder exhibits both elastic and viscous components of response and displays a temperature-, time-, and history-dependent relationship between applied stresses and resultant strains. 1,2 However, within the LVE region of response, the interrelation between stress and strain is influenced by temperature, loading history, and time alone, not by the magnitude of the stress (i.e., deformation at any time and temperature is directly proportional to the applied load). In addition, as asphalt binder is responsible for the viscoelastic behavior of all asphalt materials, it plays a dominant role in defining many of the aspects of asphalt road performance such as strength and stiffness, permanent deformation, and cracking.

Various techniques and methodologies exist to measure the rheological (viscoelastic) properties of asphalt binders including dynamic mechanical analysis using oscillatory testing generally by means of a dynamic shear [69] rheometer (DSR).⁴⁻⁶ The principal viscoelastic parameters that are obtained from the DSR are the complex shear modulus (G^*) and the phase angle (δ). Absolute value of G^* ($|G^*|$) is defined as the ratio of maximum (shear) stress to maximum strain and provides a measure of the total resistance to deformation (stiffness) when the bitumen is subjected to shear loading. G* contains elastic and viscous components that are defined as the storage modulus (G') and loss modulus (G''), respectively. These two components are related to the complex modulus and to each other through the phase (or loss) angle (δ), which is the phase, or time, lag between the applied shear stress and shear strain responses during a test. The phase angle is a measure of the viscoelastic balance of the material behavior, with extreme values of 90° corresponding to purely viscous response and 0° to purely elastic behavior, and provides an indication of the potential stress relaxation of the material. Between these two extremes, the material behavior can be considered viscoelastic in nature with a combination of viscous and elastic responses. Unlike oscillatory shear testing of binders, asphalt mixture complex modulus is typically measured in extensional mode through uniaxial loading on a cylindrical specimen; the outcome of this test is either one- or three-dimensional LVE characterization in the form of either complex modulus (E^*) or both E^* and ν^* (where ν^* is complex Poisson's ratio).

One of the primary techniques used in analyzing dynamic oscillatory data involves the construction of master curves using the interrelationship between temperature and frequency (time) to produce a continuous rheological parameter curve at a reduced frequency or time scale. The principle used to relate the equivalency between time and temperature and thereby produce a master curve is known as the time-temperature superposition principle or the method of reduced variables. The production of a smooth, continuous master curve generally relies on the asphalt binder exhibiting simple rheological behavior, termed or classified as "thermorheological simplicity." An alternative to the production of master curves is to present the rheological data in the form of a Black Space diagram. Black Space provides a two-dimensional representation of the two fundamental characteristics of LVE response, namely the norm of complex modulus ($|G^*|$ or $|E^*|$) and the phase angle (δ) , at each of the temperatures and loading frequencies at which these parameters are measured. This twodimensional representation allows for easy visualization of a material's response in the context of its stiffness as well as relaxation capabilities and more importantly, the interplay between them at any given loading frequency or temperature.

Airey demonstrated how Black Space could be used to not only represent the viscoelastic properties of different asphalt materials as an alternative to master curves and isochronal and isothermal plots, but also how to use Black Space to identify testing issues with the rheological data, performance issues with the rheological data, or both. Black Space was used to help identify compliance (testing) errors in rheological data associated with the inappropriate use of various DSR spindle geometries. Black Space diagrams were also shown to be an extremely powerful means of tracking the rheological changes in asphalt binders associated with both shortand long-term aging as well as means of studying the rheological properties of complex binders such as modified binders. Since then, the use of Black Space has been explored by a number of researchers.

This paper describes selected recent developments in the use of Black Space diagrams as a means of assessing the performance of distress mechanisms associated with asphalt materials in the following ways: the use of Black Space in aiding the interpretation and understanding of key areas consisting of damage and healing assessment of asphalt materials; the use of rheological parameters to assess cracking susceptibility; and finally, the rheological characterization of alternative binders are described with reference to prominent studies in each of these areas. It is important to note that the paper is not intended to be a comprehensive review of all the possible uses of Black Space in asphalt technology literature and is simply an overview of some key examples, specifically those focusing on newer techniques to leverage Black Space for improved asphalt material performance and increased level of sustainability.

82

83

84

85

86

87

88

89

90

91

92

93

95

96

97

98

99

104

Rheological Assessment of Global Damage and Healing

Black Space diagrams have been successfully used to provide a framework for the interpretation of experimental results from cyclic loading and fatigue tests.^{8,9} Using Black Space, changes that induce complex modulus variations during loading can be investigated based on different physical phenomena including nonlinearity, selfheating, thixotropy, and damage. Some of these can be considered reversible and therefore produce biasing effects with respect to damage analysis.

NONLINEARITY EFFECTS 94

During fatigue tests, nonlinearity can be observed on the complex modulus at the beginning of cyclic loading where at a fixed temperature and frequency, the measured complex modulus depends on the applied axial strain amplitude. This alteration in complex modulus is instantaneous and reversible. This phenomenon can be studied independently from damage effects provided that the number of cycles remains low.

An example of nonlinearity effects on complex modulus is given in figure 1 where the nonlinearity effect on asphalt mixtures was studied by means of cyclic loading tests where strain amplitude was increased and then 100 decreased, linearly, from 10 µm/m to 110 µm/m. During the test, temperatures ranged from 8°C to 14°C and 101 frequencies from 0.3 to 10 Hz. 10 Inside this narrow range, the nonlinearity direction determined on the Black 102 Space diagram was not found to be constant, although variations were small. 103

THIXOTROPY AND LOCALIZED HEATING EFFECTS

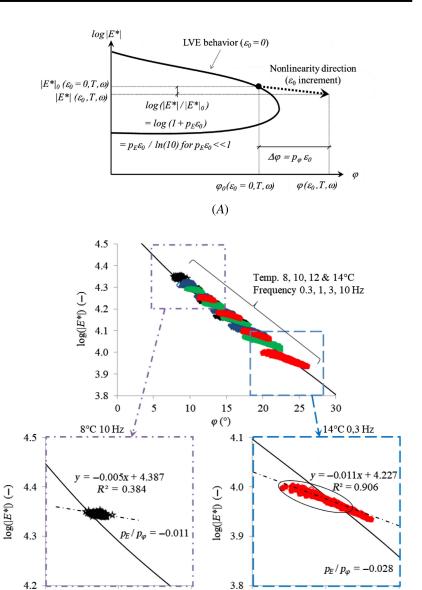
Self-heating (as well as self-cooling during rest periods) will also affect the complex modulus during cyclic loading 105 because of viscous behavior causing heat dissipation. Asphalt materials are thermosensitive; therefore, changes in 106 complex modulus occur during loading because of self-heating temperature increases. During rest periods, the 107 specimen temperature will tend to initially increase and then subsequently decrease. The change in complex 108 modulus because of temperature variation is once again reversible. 109

Thixotropy effects on the complex modulus are observed during loading and resting and defined as 110 a progressive decrease in modulus with time under loading and a gradual recovery when loading is removed 111 at a constant temperature. A classical explanation for this phenomenon is the buildup or the destruction of 112 a structural network in the material under loading and resting. During loading, stiffness tends to decrease, while 113 during rest periods it increases up to an equilibrium value with the phenomenon being reversible. Finally, damage 114 affects the complex modulus during loading with material cross-section reducing (microcracks) and a subsequent 115 reduction in stiffness. With damage accumulation, microcracks may coalesce into a macrocrack resulting in the 116 eventual material failure with this phenomenon being irreversible.

The evolution of complex modulus during cyclic loading and rest periods can be investigated in complex 118 representations such as Black Space diagrams. Figure 2 represents an example of test results and an interpretation of the evolution of the effects of each of the phenomena described above. In Black Space, it is seen that each 120 phenomenon presents a particular direction of complex modulus evolution. Before performing the continuous 121 cyclic loading test, information on temperature-sensitivity may be obtained from classical complex modulus tests. 122 If these tests include different strain amplitudes, nonlinearity effects can also be calculated. 123

FIG. 1

(A) Scheme of nonlinearity direction in Black Space and definition of p_E and $p\phi$ coefficients used to quantify the effects of nonlinearity on complex modulus (norm and phase angle respectively) and (B) results obtained from nonlinearity tests (linear increase and decrease of the amplitude of strainloading cycles from 10 to 110 μ m/m) at different temperatures and frequencies.10



To observe damage, tests with loading and rest periods should be undertaken. After each rest period, the 124 complex modulus can be compared with its initial value. Obviously, the comparison should consider the potential 125 nonlinearity effects (strain amplitude) as well as temperature effects. Some cracks developed during loading could 126 also heal during rest periods and make the damage evaluation false. However, the healing phenomenon is expected to occur more slowly than other reversible effects (temperature and thixotropy).

10

 φ (°)

15

(*B*)

18

23

 φ (°)

28

128

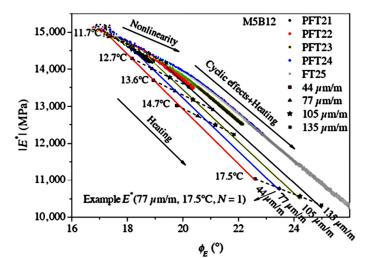
5

Babadopulos et al.¹¹ suggested that damage should have no effect (or negligible effect) on phase angle. Phase 129 angle recovers quickly during rest periods, which indicates that its change is mainly because of reversible effects 130 (temperature and thixotropy). Loading and rest periods tests were performed on bitumen to differentiate each of 131 these effects as shown in figure 3, where after 10,000 cycles of loading at a 2 % shear-strain amplitude, specimens 132

FIG. 2
Directions of different phenomena on Black

Space9: example of

experimental results.



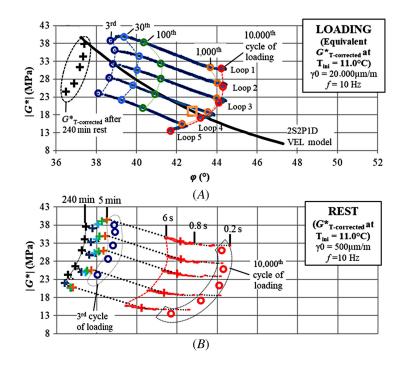
were provided with 4-h rest periods. During the rest periods, complex modulus was measured intermittently with 0.05 % strain amplitude cycles. To separate the different effects, data were corrected from temperature evolution 134 effects and plotted in figure 3 at a fixed temperature (T_{ini}) of 11°C. 135

The nonlinearity effect is visible between the complex modulus measured at low strain at the end of the rest periods and the complex modulus measured (after three cycles) at high amplitude at the beginning of the next loading period. The damage created by the loading periods can be seen as the difference between low-strain complex modulus measured at the end of the rest periods. Considering experimental fluctuations, phase angle 139

FIG. 3

test results corrected from temperature effects at $T_{ini} = 11^{\circ}$ C on bitumen represented in Black space: (A) equivalent complex shear modulus evolution during each loading period, measured at 2 % shear-strain amplitude and (B) complex modulus evolution, during each rest period of 4 h, measured at 0.05 % shear-strain amplitude (from Babadopulos et al. 11).

Loading and rest periods



149

158

169

can be considered as a constant while the norm of complex modulus decreases after each loop. The evolution 140 during loading periods is because of damage but also thixotropy. After correcting for damage, the results from the 141 Black Space diagram show the different directions of nonlinearity and thixotropy. 142

Rheological Assessment of Cracking Distress

In addition to the use of Black Space to assess asphalt material damage and healing and other physical phenom- 144 ena, it is also possible to use these diagrams to identify critical limits associated with different forms of material 145 cracking. Various rheological parameters can be defined and graphically displayed in Black space to allow critical 146 and failure regions of cracking response to be identified and material changes with regard to aging and rejuvenation to be mapped. 148

THERMAL CRACKING - BENDING BEAM RHEOMETER DATA BLACK SPACE

The development of the S and m criteria for thermal cracking was validated by inspection of built pavements by 150 Leahy, Harrigan, and Von Quintus. 12 Subsequently, Rowe 13 showed how the S and m criteria could then be 151translated to $|G^*|$ and phase angle using a transformation method by fitting a discrete spectrum to the bending 152 beam rheometer (BBR) data and performing an interconversion to the dynamic properties. 153

Once the data are transformed, it is then possible to take the criteria and insert these into Black Space where C11 the limiting criteria become a value of $|G^*|$ (111 MPa) and phase lag, δ (26.2°) at a frequency of 0.0167 radians/s 155 (1/60 s), that correspond to the S and m values (at 60 s) as shown in figure 4. Thus, we observe that the S and m 156 criteria are essentially the same as the specification of a modulus and phase angle in the Black space. 157

DURABILITY CRACKING - GLOVER-ROWE PARAMETER

One approach to assess the cracking resistance of asphalt materials, particularly durability cracking, is through the 159 use of Black Space diagrams and a point parameter known as the Glover-Rowe (G-R) parameter. Based initially on 160 the relationship between ductility and pavement performance and an understanding of the importance of the 161 stress relaxation properties of the binder in an asphalt mixture, the G-R parameter can be used to evaluate the 162 resistance of binder and asphalt mixtures to age-related cracking. 14-16 The G-R parameter for binders can 163 be computed from measurements of complex modulus ($|G^*|$) and phase angle (δ) using a DSR at a frequency 164 of 0.005 rad/s and 15°C using equation (1). 165

$$G - R = |G*|(\cos \delta)^2 / \sin \delta \tag{1}$$

By plotting the G-R parameter and including the limiting values associated with a warning of the probability 166 of cracking (180 kPa) and presence of significant cracking (600 kPa) (values derived from field durability cracking 167 evaluation¹⁴), it is possible to identify the effect of aging on the susceptibility of a binder to durability cracking as 168 shown in figure 5.

Similarly, the same concept can also be considered for rejuvenation as shown in figure 6 for two locations 170 treated with a rejuvenator. 17

Figure 6 also shows lines that represent the rheological index (R-value) as defined by the Christensen-Anderson (CA) model¹⁸ with a glassy modulus (G_g) set as 1 GPa. However, this assumption that the value 173 of G_{v} is equal to 1 GPa for all binders is most likely incorrect. Other works have shown that this value can vary 174 considerably and also changes with temperature susceptibility of the binder. Thus, the assumption that R = 1759-log G_{c} , where G_{c} is the crossover modulus is incorrect, and it has been suggested that it is better to simply use the 176 value of G_c as a specification parameter rather than R. G_c has the advantage in that it lies in a similar stiffness range 177 to the G-R value for most paving binders and effectively characterizes the shape of the master curve in the high 178 stiffness region whereas the G-R value identifies the hardness of the binder. Other parameters being considered 179 for specifications in the intermediate temperature/non-load related cracking region also include the phase angle 180

FIG. 4 Black Space data for BBR results interconverted to dynamic data (zero, low, medium, and high indicate level of field cracking).

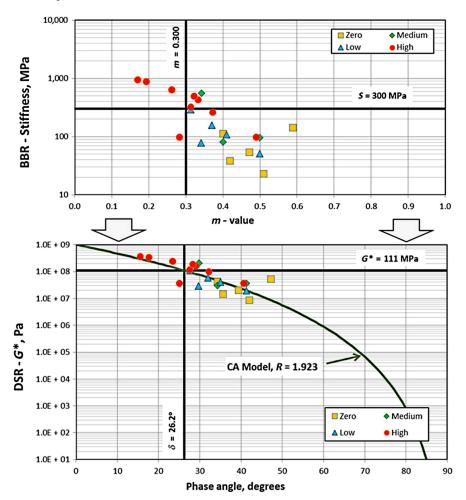
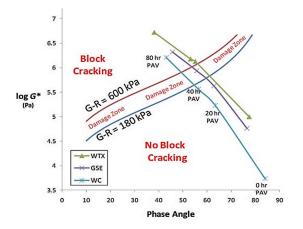


FIG. 5Black Space diagram including *G-R* parameter limits. Different binders at different stages of aging. ¹⁷

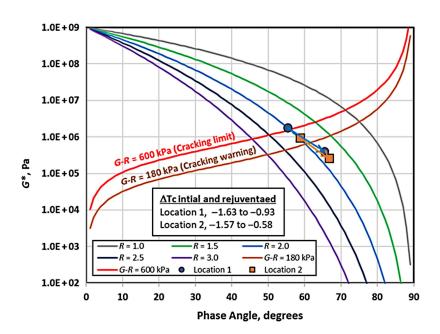


202

203

FIG. 6

Black Space diagram including G-R parameter limits Treatment of binders with rejuvenators (other rheological indices, ΔT_c and R-values also shown).17



response at a stiffness of 8,967 kPa, $\delta_{G^*=8.967~\text{GPa}}$. It should be noted that this parameter, the *R*-value, the G_c and 181 ΔT_c (shape parameter determined as the difference between the critical temperatures of $T_{stiffness~(60~s)}$ and $T_{m-value}$ 182 (60 s) from the BBR) all define the shape of the master curve in the intermediate temperature region, much in the 183 same manner that the penetration index or penetration-viscosity number would characterize properties using 184 empirical specification approaches.

By inspection of the data in figure 6, we note that at an R-value of 2, the value of $|G^*|$ is close to a value of 186 1 MPa at the critical region where the G-R parameter transitions from a "cracking warning" condition to a "cracking limit" condition. Several approaches exist for understanding the stiffness and relation properties in this 188 stiffness range. Regardless, we note that it is important that both stiffness and relation properties are defined 189 in this region. The advantage of the G-R parameter to other parameters is that as materials age, the relationship 190 produced intersects with the G-R lines at nearly a right angle, indicating that the parameter is very sensitive to the 191 changes in the properties that are occurring because of aging.

As discussed earlier, the rheological index (*R*-value) as defined by the CA model, $^{18}\delta_{G^*=8.967~\text{GPa}}$, $G_{\mathcal{O}}$ and $\Delta T_{\mathcal{O}}$ 193 effectively define the shape of the master curve in the higher stiffness region ($|G^*| \ge 10^5$ Pa). The selection 194 of a parameter for specification use should depend upon the ease of measurement (likely to significantly affect 195 implementation) and the accuracy of testing as determined by interlaboratory studies (precision, repeatability, 196 reproducibility, etc.). However, while the shape of the master curve is of considerable importance, the relative 197 hardness (stiffness) is needed. This can be captured by the G-R parameter, which can be regarded as a "point" 198 parameter. Other parameters that effectively capture the hardness of the material include the crossover frequency, 199 ω_{cp} (reference temperature must be specified) or the temperature at which the crossover modulus occurs, T_{cr} or 200 T_{VET} (frequency must be specified). However, these last two parameters cannot be easily plotted in Black Space, 201 and the conceptual tie with performance is more difficult to visualize.

DURABILITY AND THERMAL CRACKING

As discussed earlier, a direct relationship exists between measurements conducted in the frequency and time 204 domain provided that strains are kept within the LVE region. For asphalt binders, we have made use of inter- 205 conversion technologies using the RHEA software and the computation of the calculated relaxation spectra fit to 206

the data. The parameters for limiting cold-temperature thermal cracking (S = 300 MPa and m = 0.300) thus can 207 be translated into values of $|G^*| = 111$ MPa and $\delta = 26.8^\circ$ at a frequency of 0.0167 radians/s (1/60 s). This intercept of complex modulus and phase lag can be shown as a G-R relationship that has a value of 184 MPa, and 209 this could be used as an alternate to the S and m values currently used as shown together with other Black Space 210 parameters in figure 7.

211

227

228

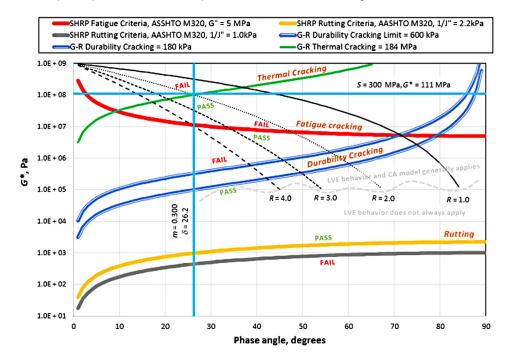
In earlier work, Anderson et al. 16 showed that a good correlation between ΔTc and the G-R parameter existed. However, because one of the parameters is a shape parameter whereas the other is a point parameter, no 213 correlation should be expected across the wide range of materials used in asphalt paving. Rowe²¹ presented data 214 that demonstrated that binders with different rheological types have significantly different behavior when comparing the G-R parameters to ΔTc . Specifically, elastomeric binders that are known to perform better with respect 216 to cracking often have low values of ΔTc .

Zhang, Sias, and Dave²² presented similar data in the format of G-R versus ΔTc that shows the relationships for different binders with G-R and ΔT_c parameters as shown in figure 8. In this study, the propensity to 219 cracking of reclaimed asphalt pavement (RAP)-modified materials used in the northeastern USA was studied 612 with binders after different aging conditions. The dashed lines represent the cracking-warning values, and 221 the solid lines represent the cracking-limit values for the two parameters. Points in the bottom right quadrant 222 of the plot are acceptable under both criteria whereas those in the top left quadrant would be sensitive to 223 cracking using both criteria. The short-term conditioned binders (first point on each line) generally fall into 224 the safe zone, which means that typically no cracking problems are expected. As the materials age, they move 225 toward the upper left quadrant, indicating that there may be significant cracking problems based on the ΔT_c 226 and G-R criteria.

FATIGUE CRACKING AND CRACKING PERFORMANCE LIMITS

In addition to representing the G-R parameter in Black Space and providing limits for the onset and failure 229 associated with durability cracking, it is also possible to represent other non-load and load-related cracking 230





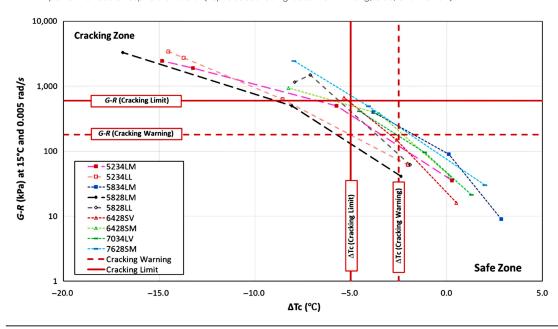


FIG. 8 Performance space diagram of G-R and ΔT_c parameters for balancing thermal and durability cracking performances of asphalt binders, (reproduced using data from Zhang, Sias, and Daye²²).

and rutting limits. The Black Space diagram can depict pass and fail limits for rutting as well as forms of pavement cracking (durability, fatigue, and thermal) as shown earlier. It should be noted that at the stiffness values consistent with rutting, the binder is generally behaving in a different manner. For example, we know that as the stiffness drops below 10⁵ Pa that the CA model loses its validity. 18

231

232

For conventional binders, ΔTc is strongly correlated with the R-value. Specifiers generally consider limits for ΔTc in specifications with values around -3.5 to -5. Values lower than this would represent binders that are excluded from specifications. The R-value of 1.92 corresponds approximately to a ΔTc value of 0. This value can 237 vary to a small extent with changes in the glassy modulus and temperature susceptibility. An R-value of 3.0 is a 238 practical limit related to a low (negative) value of ΔTc of around -5.0. This value of R is typical of an oxidized or 239 aged binder and represents a temperature susceptibility defined by ΔTc in the critical range. A low R-value 240 represents a binder that is not practical because the material will generally have a high temperature susceptibility. 241 Thus, conventional asphalt binders will lie within the shaded area as shown in figure 9.

The specification of an R-value is problematic because this parameter is not easily determined and is a 243 function of the analysis method. However, if a constant value of 1 GPa is assumed for the glassy modulus, 244 the control of the R-value can be directly correlated to the crossover modulus, G_c , (the value of $|G^*|$ at a phase 245 angle of 45°), which can be easily measured for paving grade binders. This effectively allows both ΔTc and G-R to 246 be controlled by Black Space parameters.

Thus, in summary for binders, the critical binder parameters associated with behavior in a Black Space plot, 248 including those developed under the SHRP program, become the following: 249

- Thermal: G-R, 184 MPa measured at a slow frequency (1/60 s) 0.0167 rads/s at T_{min} + 10C or $-|G^*|$ < AQ7 111 MPa and $\delta > 26.2^{\circ}$ at the same conditions.
- Fatigue (SHRP): |G*|sinδ measured at 10 rads/s at intermediate temperature parameter as developed by SHRP researchers, which is under review.
- Durability: G-R parameter measured at 15°C and 0.005 rads/s with two criteria being considered (180 kPa and 600 kPa) and Gc > 1 MPa, which effectively removes the need to specify ΔTc .

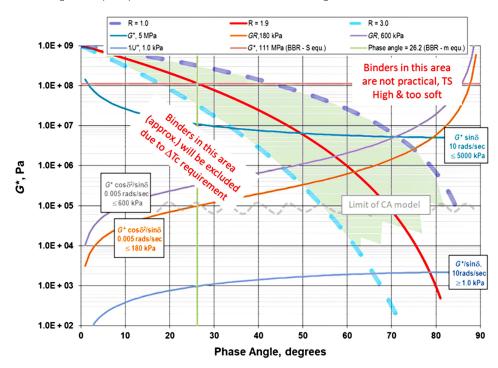


FIG. 9 Extending Black Space parameters with limits associated with ranges in ΔTc .

Deformation: $|G^*| / \sin \delta (1/J^*)$ as currently used – but now because of nonlinear effects, it is proposed that 256 the multiple stress creep recovery test will be a better test

C14

258

266

G-R CONCEPT FOR ASPHALT MIXTURES

Based on the binder G-R approach, Mensching, Rowe, and Daniel²³ developed the mixture Glover-Rowe (G- R_m) 259 parameter using stiffness and phase angle measured on the asphalt mixture ($|E^*|$ and δ). However, determining a 260 suitable temperature and frequency to calculate $G-R_m$ has required considerable research effort. Oshone et al. 24 261 used results from 81 asphalt mixtures to assess different temperature and frequency combinations (fig. 10). This 262 work observed that most discrimination between mixtures in terms of $|E^*|$ and phase angle was observed at 15°C 263 and $\frac{1}{2}$ a Subsequent research has further developed $G-R_m$ to use a commonly measured temperature-frequency combination of 20°C and 5 Hz.25,26

Oshone et al. 24 further conducted Pearson's correlation analysis on the $G-R_m$ parameter (15°C and 5 rad/s) 267 from the 81 asphalt mixtures. As expected, the binder content and voids in mineral aggregate showed strong 268 correlations where an increase in these parameters results in lowering of G-R_m. PGLT also showed a strong 269 correlation where with lowering of PGLT, the $G-R_m$ reduces (in other words, a better PGLT lowers the value 270 of $G-R_m$). Increasing nominal maximum aggregate size for mixtures increases $G-R_m$, and increasing amounts of 271 RAP as well as PG high-temperature grade increases $G-R_m$ but with a smaller degree of correlation.

 $G-R_m$ can be used to compare various mixtures (binder grades, recycled material content, etc.) and to evaluate and quantify changes in viscoelastic material properties with aging (e.g., fig. 11) or with rejuvenation. Kaseer 274 et al.²⁷ used mixture Black Space and the $G-R_m$ parameter to evaluate various strategies for producing mixtures 275 with higher RAP contents. Various recycling agents and use of a softer virgin binder were also evaluated at both 276 short- and long-term aging conditions. Zhang, Sias, and Dave²² used the $G-R_m$ to correlate laboratory conditioning methods with field-aging durations for a set of mixtures. Zhang²⁸ also developed a rheology-based mixture 278

283

FIG. 10

Discrimination between mixtures in terms of $|E^*|$ and phase angle at different frequency and temperature combinations (reproduced using data from Oshone et al.24).

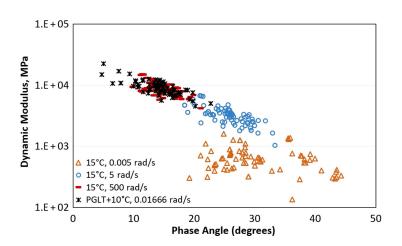
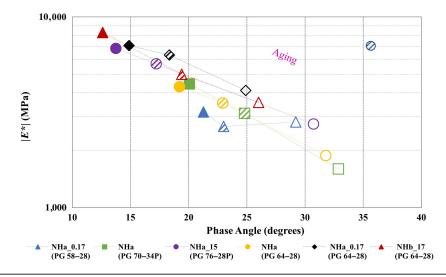


FIG. 11 Mixture G-R parameter evolution with aging (from Ogbo et al. 26).

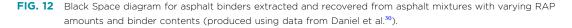


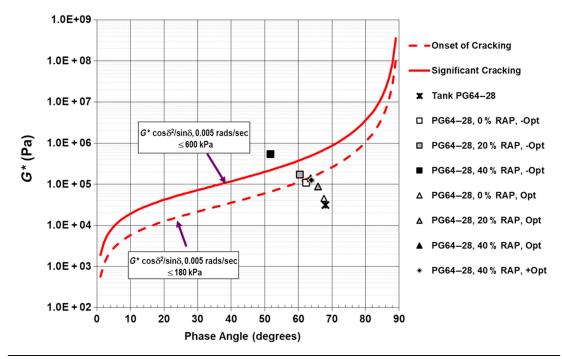
aging model using the G-R_m parameter to evaluate cracking and aging susceptibility of mixtures with different 279 binder grades and RAP content.

Master curve shape parameters obtained from fitting mixture $|E^*|$ and phase angle master curves are also 281 used to track and quantify the impact of aging and rejuvenation on the mixture viscoelastic properties.²⁹ 282

EVALUATING RECYCLED MATERIALS, AGING, AND REJUVENATION

Recycled asphalt content in asphalt binders and mixtures have prominent effects on their rheological properties. 284 A study by Daniel et al.³⁰ extensively evaluated effects of RAP content on Black Space parameters. An example 285 result from that research is presented in figure 12 and shows the Black Space diagram (along with G-R parameter 286 limits) for extracted and recovered binders from plant-produced mixtures as a function of RAP content (0, 20, 287 and 40 % by total weight of mix) and binder amount (optimum, optimum -0.5 %, and optimum +0.5 %). Results 288 for tank binder used in production are also shown in the figure for comparison. The results show that increasing 289





the RAP amount and decreasing binder content led to significant increases in binder stiffness and loss of phase 290 angle with higher RAP mixtures (40 % RAP) all in the "crack warning" region for the G-R parameter and the lowasphalt content mixture with high RAP amount past the cracking limit. The effect of lowering binder content on 292 the G-R parameter can be attributed to decreases in asphalt binder film thickness and thus increased aging during 293 mix production.

Data from the same study by Daniel et al.³⁰ also include assessment of R-value and crossover frequency for 295 the binders extracted from asphalt mixtures with varying RAP amounts and binder contents. As expected, introduction of RAP in the mixture results in a significant reduction in crossover frequency. While RAP amount 297 increases from 20 to 40 %, the R-value increases, with this effect being more pronounced for mixtures with a lower 298 binder content.

Black Space and the G-R parameter can also be used to access both the aging and rejuvenating effects linked 300 with binders associated with recycled asphalt pavements. Rahbar-Rastegar, Daniel, and Dave³¹ used mixture 301 Black Space to compare various laboratory conditioning protocols for mixtures and to evaluate how both 302 $|E^*|$ and phase angle master curves change with aging.

303

307

312

Figure 13 shows an example of the evolution of the G-R parameter (measured on extracted and recovered 304 binders) with mixture-aging conditions. In this study, Zhang, Sias, and Dave²² used this analysis to determine the 305 mixture-aging condition that corresponds to the standard 20-h pressure aging vessel aging on the virgin binder C15 and also to evaluate the change in aging with depth using measurements from field cores.

The extent of virgin and RAP binder blending is presented in figure 14 with short-term and long-term 308 aging conditions (indicated by the rolling thin-film oven test and pressure aging vessel).³² The Black C16 Space diagram shows the effect of different degrees of binder activation, as a measure of virgin and RAP binder 310 blending, and the shift toward the top left-hand corner with aging and in the opposite direction with 311 rejuvenation.

319

325

FIG. 13 Evolution of G-R parameter with aging for virgin and extracted and recovered binders.²²

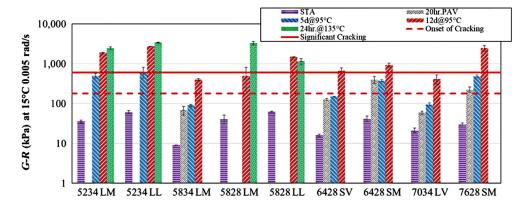
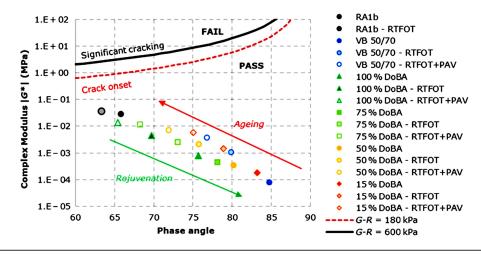


FIG. 14 G-R parameter for recycled binders showing aging and rejuvenating effects. 32

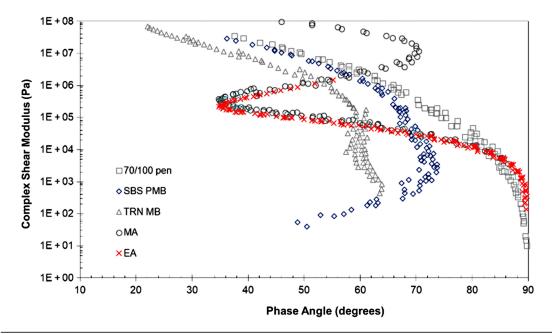


The effect of different types of recycling agents can also be compared using Black Space and the G-R parameter. Work by Bajaj et al.³³ showed how different types or categories of recycling agents produce primarily softening effects (reduction in $|G^*|$ only) or rejuvenating effects (reduction in $|G^*|$ and increase in phase angle). This 315 study also evaluated the impact of different conditioning sequences on the rheological parameters of binders 316 blended with RAP and recycling agents to examine how the interactions between the different materials impact 317 rheological changes with aging.

Rheological Assessment of Alternative Binders

The techniques and approaches that have made use of Black Space have generally been applied to conventional 320 asphalt materials. However, the move toward more sustainable solutions to minimize environmental impact has 321 resulted in increased use of industrial byproducts and wastes in asphalt mixtures with the idea of partially replacing asphalt binders with bio-based materials or alternative binders. These synthetic binders or bio-based materials 323 (also known as bio-binders or bio-oils) can be considered as renewable materials as compared to conventional 324 asphalt binders that are derived from fossil fuels.34-36

FIG. 15 Black Space diagram of rheological data for different conventional (70/100 pen), polymer-modified (SBS PMB) tire rubber-modified (TRN MB), and synthetic binders (MA, EA) (after Airev et al. 44),



Most of these renewable bio-based materials are of vegetative origin such as lignin, tall oil, pitch, wood resins, 326 and plant sap. 35 Another widely used renewable material of vegetative origin is waste cooking oil, which is available in 327 large quantities all over the world. 37,38 Further examples are bio-oils obtained from vegetable oils and biomass such as 328 soy, linseed, and rapeseed. Other sources of bio-binders include algae,³⁹ wood residues,^{40–42} and swine manure.⁴³ 329

Another aspect to be considered is the complexity of the treatment before the employment of these renewable materials. Most bio-based materials used for asphalt materials are obtained from raw materials through 331 thermal treatments, chemical treatments, or both, such as pyrolysis, esterification, and hydrothermal liquefaction. 332 These production techniques add an extra dimension to the rheological complexity of the final binder.

Black Space diagrams can be considered to provide rheological "fingerprints" for these different binders and 334 have been used in figure 15 to provide a convenient method of comparing different categories of binders such as 335 standard paving grade binders, modified binders, and synthetic polyacrylate binders. 34,44 The Black Space curves 336 allow the unique rheological behavior of the polyacrylate binders to be illustrated without the need for more 337 advanced rheological characterization involved with the generation of master curves.

Black Space diagrams have also been used for bio-binders produced using lignin and sawdust and produced 339 using pyrolysis and hydrothermal liquefaction procedures at different operating conditions. Similar to the rheological behavior shown in figure 15, the rheological Black Space curves can be used to show the unique viscoelastic 341 properties of these bio-based materials. 342

338

343

348

Concluding Remarks

The paper has described three broad applications of the use of Black Space diagrams in terms of the rheological 344 assessment of asphalt binders and mixtures to aid interpretation and analysis of material and pavement performance. These three applications included global damage and healing assessment, rheological characterization for 346 cracking behavior evaluation (including effects of recycled materials, aging, and rejuvenation), and rheological 347 fingerprinting of alternative synthetic or bio-based sustainable asphalt binders.

Journal of Testing and Evaluation

380

381

382 C17

385

387

389

C18

392

In terms of cyclic loading and fatigue tests, Black Space diagrams have been used to evaluate the damage and 349 healing changes in complex modulus and phase angle through the selection of strain amplitude sweep tests as well 350 as combination loading and rest period cyclic tests. The results from these Black Space diagrams have enabled 351 nonlinearity as well as the phenomena of self-heating and thixotrophy to be identified in addition to changes in 352 complex modulus and phase angle because of damage and healing.

In terms of low-temperature (thermal) cracking, it is possible to transform the Superpave S (300 MPa) and 354 m (0.3) criteria to a limited complex modulus (111 MPa) and phase angle (26.2°) set of criteria at a frequency of 355 0.0167 radians/s with these limits being used in Black Space to identify regions of high or low thermal-cracking 356 susceptibility.

Black Space diagrams and a point parameter known as the G-R parameter have been successfully used to 358 assess the durability (age-related) cracking resistance of asphalt materials. The G-R parameter, together with 359 limiting values associated with a warning of the probability of cracking (180 kPa) and presence of significant 360 cracking (600 kPa), can be presented in Black Space to monitor the susceptibility of asphalt binders to aging 361 as well as the reverse effect of rejuvenation. 362

With the ability to transform the thermal cracking criteria of S and m to G^* and δ , it is also possible to link 363 thermal cracking with durability cracking by defining a G-R value of 184 MPa for thermal cracking. Although not 364 a direct correlation, it is also possible to link the G-R parameter and ΔTc to identify asphalt materials that have 365 a greater or lower potential for significant cracking.

In addition to durability cracking, the Black Space diagram can also depict pass and fail limits for rutting 367 as well as various forms of non-load and load-relating pavement cracking. It is also possible to establish relationships between ΔTc , R-value, and the G-R parameter and provide a shaded area in the Black Space diagram for 369 conventional asphalt binders.

It is also possible to extend the G-R parameter to asphalt mixtures (G- $R_m)$ with most measurements made at 371 a temperature-frequency combination of 20°C and 5 Hz. The $G-R_m$ parameter can then be used to evaluate 372 and quantify changes in viscoelastic material properties with aging or with rejuvenation. Black Space and the 373 $G-R_m$ parameter are also used to assess the cracking and aging susceptibility of asphalt mixtures with different 374 contents and types of RAP.

Finally, Black Space has been used to illustrate the complex rheological response of both synthetic binders 376 and bio-binders with some of these binders showing useful combinations of high stiffness as well as good 377 relaxation capabilities.

References 379

- J. D. Ferry, Viscoelastic Properties of Polymers (New York: John Wiley and Sons, 1980).
- H. A. Barnes, J. F. Hutton, and K. Walters, An Introduction to Rheology (Amsterdam: Elsevier, 1989).
- C. Van der Poel, "A General System Describing the Visco-Elastic Properties of Bitumen and Its Relation to Routine Test Data," Journal of Applied Chemistry 4, no. 5 (May 1954): 221-236, https://doi.org/10.1002/jctb.5010040501
- H. S. Pink, R. E. Merz, and D. S. Bosniack, "Asphalt Rheology: Experimental Determination of Dynamic Moduli at Low 384 Temperature," Association of Asphalt Paving Technologists 49 (1980): 64-94.
- J. L. Goodrich, "Asphalt and Polymer Modified Asphalt Properties Related to the Performance of Asphaltic Concrete 386 Mixes," Association of Asphalt Paving Technologists 57 (1988): 116-175.
- J. C. Petersen, R. E. Robertson, J. F. Branthaver, P. M. Harnsberger, J. J. Duvall, S. S. Kim, D. A. Anderson, et al., Binder 388 Characterization and Evaluation. Volume 4: Test Methods, SHRP-A-370 (Washington, DC: Strategic Highway Research Program, National Research Council, 1994).
- G. D. Airey, "Use of Black Diagrams to Identify Inconsistencies in Rheological Data," International Journal of Road 391 Materials and Pavement Design 3, no. 4 (2002): 403-424, https://doi.org/10.1080/14680629.2002.9689933
- S. Mangiafico, "Linear Viscoelastic Properties and Fatigue of Bituminous Mixtures Produced with Reclaimed Asphalt 393 Pavement and Corresponding Binder Blends" (PhD diss., École Nationale des Travaux Publics de l'État (ENTPE) de 395 l'Université de Lyon (UdL), Vaulx-en-Velin, 2014).
- Q. T. Nguyen, "Comportement thermomécanique des enrobés bitumineux sous solicitations cycliques dans les domaines 396 linéaire et non-linéaire" (PhD diss., École Nationale des Travaux Publics de l'État (ENTPE) de l'Université de Lyon (UdL), 397 Vaulx-en-Velin, 2011). 398

- S. Mangiafico, L. F. A. L. Babadopulos, C. Sauzéat, and H. Di Benedetto, "Nonlinearity of Bituminous Mixtures," Mechanics of Time-Dependent Materials 22 (2018): 29-49, https://doi.org/10.1007/s11043-017-9350-3
- 11. L. F. A. L. Babadopulos, G. Orozco, C. Sauzéat, and H. Di Benedetto, "Reversible Phenomena and Fatigue Damage during 401 Cyclic Loading and Rest Periods on Bitumen," International Journal of Fatigue 124 (July 2019): 303-314, https://doi.org/ 402 403 10.1016/j.ijfatigue.2019.03.008
- R. B. Leahy, E. T. Harrigan, and H. Von Quintus, Validation of Relationships Between Specification Properties and 404 Performance, SHRP-A-409 (Washington, DC: Strategic Highway Research Program, National Research Council, 1994). 405
- G. M. Rowe, "Interrelationships in Rheology for Asphalt Binder Specifications," in Proceedings of the Fifty-Ninth Annual 406 Conference of the Canadian Technical Asphalt Association (CTAA): Winnipeg, Manitoba (Victoria, Canada: Canadian 407 408 Technical Asphalt Association (CTAA), 2014), 457–483.
- C. J. Glover, R. R. Davison, C. H. Domke, Y. Ruan, P. Juristyarini, D. B. Knorr, and S. H. Jung, Development of a New 409 Method for Assessing Asphalt Binder Durability with Field Evaluation, FHWA/TX-05/1872-2 (Austin, Texas: Texas 410 Department of transportation, Research and Technology Implementation Office, 2005). 411
- G. King, M. Anderson, D. Hanson, and P. Blankenship, "Using Black Space Diagrams to Predict Age-Induced Cracking," in Seventh RILEM International Conference on Cracking in Pavements (Paris: The International Union of Laboratories 413 and Experts in Construction Materials, Systems and Structures (RILEM), 2012), 453-463, https://doi.org/10.1007/978-94-007-4566-7 44
- R. M. Anderson, G. N. King, D. I. Hanson, and P. B. Blankenship, "Evaluation of the Relationship between Asphalt Binder 416 Properties and Non-Load Related Cracking," Journal of the Association of Asphalt Paving Technologists 80, (2011): 615-

C20

420 C21

423

AQ10

C22

C25

- G. M. Rowe, "The Development of the Delta Tc and Glover-Rowe Parameters for the Control of Non-Load Associated 419 17. Cracking" (paper presentation, 12th Conference on Asphalt Pavements for Southern Africa, Sun City, South Africa, October 13-16, 2019).
- 18. D. W. Christensen and D. A. Anderson, "Interpretation of Dynamic Mechanical Test Data for Paving Grade Asphalt 422 Cements," Association of Asphalt Paving Technologists 61 (1992): 67–116.
- 424 G. R. Dobson, "The Dynamic Mechanical Properties of Bitumen," Association of Asphalt Paving Technologists 38 425 (February 1969): 123-139.
- P. Kris, G. Reinke, and M. Anderson, "Asphalt Institute DSR-PF TF Outcomes & Recommendations" (presentation, June 426
- 21. G. M. Rowe, "New Methods for Assessing Rheology Data Such as Δtc and G-R Parameter and Their Relationship to 428 Performance of REOB in Asphalt Binders and Other Materials," (presentation, Asphalt Mix and Binder ETG Meeting, Ames, Iowa, 2017).
- 22. R. Zhang, J. E. Sias, and E. V. Dave, "Correlating Laboratory Conditioning with Field Aging for Asphalt using Rheological 431 Parameters," Transportation Research Record: Journal of the Transportation Research Board 2674, no. 5 (April 2020): 393-432 404, https://doi.org/10.1177/0361198120915894 433
- 23. D. J. Mensching, G. M. Rowe, and J. S. Daniel, "A Mixture-Based Black Space Parameter for Low-Temperature 434 Performance of Hot Mixture Asphalt," International Journal of Road Materials and Pavement Design 18, no. 1 435 (2017): 404–425, https://doi.org/10.1080/14680629.2016.1266770 436
- 24. M. Oshone, D. Ghosh, E. V. Dave, J. S. Daniel, J. M. Voels, and S. Dai, "Effect of Mix Design Variables on Thermal 437 Cracking Performance Parameters of Asphalt Mixtures," Transportation Research Record: Journal of the 438 Transportation Research Board 2672, no. 28 (September 2018): 471-480. https://doi.org/10.1177/0361198118797826
- 25. A. Epps Martin, F. Kaseer, E. Arámbula-Mercado, A. Bajaj, J. S. Daniel, E. Hajj, N. Morian, and C. Ogbo, "Component 440 Materials Selection Guidelines and Evaluation Tools for Binder Blends and Mixtures with High Recycled Materials 441 Content and Recycling Agents," Association of Asphalt Paving Technologists 88 (2019): 1-35.
- C. Ogbo, F. Kaseer, M. Oshone, J. E. Sias, A. Epps Martin, "Mixture-Based Rheological Evaluation Tool for Cracking in 443 Asphalt Pavements," International Journal of Road Materials and Pavement Design 20, no. 1 (March 2019): S299-S314, 444 https://doi.org/10.1080/14680629.2019.1592010 445
- 27. F. Kaseer, A. Bajaj, A. Epps Martin, E. Arámbula-Mercado, and E. Y. Hajj, "Strategies for Producing Asphalt Mixtures 446 with High RAP Content," Journal of Materials in Civil Engineering 31, no. 11 (November 2019): 05019002, https://doi. org/10.1061/(ASCE)MT.1943-5533.0002910
- R. Zhang, "Evaluation and Identification of Cracking Susceptibility of Asphalt Binders and Mixtures by Incorporation of 449 Effects of Aging on Performance" (PhD diss., University of New Hampshire, 2020). 450
- M. Oshone, J. E. Sias, E. V. Dave, A. Epps Martin, F. Kaseer, and R. Rahbar-Rastegar, "Exploring Master Curve Parameters 451 to Distinguish between Mix Variables," International Journal of Road Materials and Pavement Design 20, no. 2 (July 452 2019): S812-S826, https://doi.org/10.1080/14680629.2019.1633784 453
- J. S. Daniel, T. Bennert, Y. R. Kim, W. Mogawer, D. Mensching, and M. Sabouri, Evaluation of Plant Produced RAP 454 Mixtures in the Northeast, TPF-5(230) (Concord, New Hampshire: New Hampshire Department of Transportation, 455 2015).
- 31. R. Rahbar-Rastegar, J. S. Daniel, and E. V. Dave, "Evaluation of Viscoelastic and Fracture Properties of Asphalt Mixtures 457 with Long-Term Laboratory Conditioning," Transportation Research Record: Journal of the Transportation Research 458 Board 2672, no. 28 (August 2018): 503-513, https://doi.org/10.1177/0361198118795012 459

32.	G. M. Pires, "A New Methodology for the Measurement of the Reclaimed Asphalt Degree of Binder Activation" (PhD	460
	thesis, University of Nottingham, 2018).	461

- A. Bajaj, A. Epps Martin, G. King, C. Glover, F. Kaseer, and E. Arámbula-Mercado, "Evaluation and Classification of Recycling Agents for Asphalt Binders," Construction and Building Materials 260 (2020): 119864, https://doi.org/10.1016/j. 464
- 34. G. D. Airey, M. H. Mohammed, and C. Fichter, "Rheological Characteristics of Synthetic Road Binders," Fuel 87, nos. 10–11 (August 2008): 1763–1775, https://doi.org/10.1016/j.fuel.2008.01.012
- L. P. Ingrassia, X. Lu, G. Ferrotti, and F. Canestrari, "Renewable Materials in Bituminous Binders and Mixtures: 467
 Speculative Pretext Or Reliable Opportunity?" Resources, Conservation, and Recycling 144 (May 2019): 209–222, 468
 https://doi.org/10.1016/j.resconrec.2019.01.034
- M. Zahoor, S. Nizamuddin, S. Madapusi, and F. Giustozzi, "Recycling Asphalt Using Waste Bio-Oil: A Review of the Production Processes, Properties and Future Perspectives," *Process Safety and Environmental Protection* 147 (March 2021): 1135–1159. https://doi.org/10.1016/j.psep.2021.01.032
- Z. Sun, J. Yi, Y. Huang, D. Feng, and C. Guo, "Properties of Asphalt Binder Modified by Bio-Oil Derived from Waste 473 Cooking Oil," Construction and Building Materials 102, Part 1 (January 2016): 496–504, https://doi.org/10.1016/j. 474 conbuildmat.2015.10.173
- H. Wen, S. Bhusal, and B. Wen, "Laboratory Evaluation of Waste Cooking Oil-Based Bioasphalt as a Sustainable Binder for Hot-Mix Asphalt," in Transportation Research Circular E-C165: Alternative Binders for Sustainable Asphalt Pavements (Washington DC: Transportation Research Board, 2012), 49–60.
- E. Chailleux, M. Audo, B. Bujoli, C. Queffelec, J. Legrand, and O. Lepine, "Alternative Binder from Microalgae: Algoroute Project," in Transportation Research Circular E-C165: Alternative Binders for Sustainable Asphalt Pavements (Washington DC: Transportation Research Board, 2012), 7–14.
- S. B. Cooper III, L. N. Mohammad, and M. Elseifi, "Evaluation of Asphalt Mixtures Containing Renewable Binder Technologies," International Journal of Pavement Research and Technology 6, no. 5 (September 2013): 570–575, 483 https://doi.org/10.6135/ijprt.org.tw/2013.6(5).570
- A. Jiménez del Barco-Carrión, M. Pérez-Martínez, A. Themeli, D. Lo Presti, P. Marsac, S. Pouget, F. Hammoum, E. 485
 Chailleux, and G. D. Airey, "Evaluation of Bio-materials' Rejuvenating Effect on Binders for High-Reclaimed 486
 Asphalt Content Mixtures," Materiales de Construcción 67, no. 327 (2017): 1–11, https://doi.org/10.3989/mc.2017.04516
 487
- J. Peralta, R. C. Williams, M. Rover, M. H. M. R. D. Silva, "Development of Rubber-Modified Fractionated Bio-Oil for Use as Noncrude Petroleum Binder in Flexible Pavements," in Transportation Research Circular E-C165: Alternative Binders for Sustainable Asphalt Pavements (Washington DC: Transportation Research Board, 2012), 23–36.
- E. H. Fini, I. L. Al-Qadi, Z. You, B, Zada, and J. Mills-Beale, "Partial Replacement of Asphalt Binder with Bio-Binder: 491
 Characterization and Modification," *International Journal of Pavement Engineering* 13, no. 6 (2012): 515–522, https://doi. 492
 org/10.1080/10298436.2011.596937
- G. D. Airey, J. R. A. Grenfell, A. Apeagyei, A. Subhy, and D. Lo Presti, "Time Dependent Viscoelastic Rheological Response of Pure, Modified and Synthetic Bituminous Binder," *Mechanics of Time-Dependent Materials* 20, no. 3 495 (2016): 455–480, https://doi.org/10.1007/s11043-016-9295-y